Influence of noise-reduction schemes on statistics of the diffusion-limited aggregation model at meso- and macroscales

Vladislav A. Bogoyavlenskiy*
Low Temperature Physics Department, Moscow State University, 119899 Moscow, Russia
(Received 1 August 2000; published 22 December 2000)

This paper is devoted to the problem of noise reduction in the diffusion-limited aggregation (DLA) model. We investigate the influence of multiple-hit averaging on statistical properties of DLA clusters at meso- and macroscopic length scales. For this purpose, we analyze the long-range correlation of the symmetry broken at the microscopic level via the introduction of a chirality to the original Witten-Sander DLA algorithm. Instead of the usual circular growth units, we consider them to consist of chiral (i.e., without inversion symmetry) combinations of microblocks. Extensive Monte Carlo simulations performed for off- and on-square-lattice conditions reveal the asymptotically achiral behavior of the model, which also occurs when one proceeds to noise-reducing DLA modifications such as multiple-hit averaging with and without erasing. This allows us to conclude that neither of the noise-reducing schemes studied breaks the original balance between deterministic and stochastic forces governing the long-range statistics of the DLA model.

DOI: 10.1103/PhysRevE.63.011602 PACS number(s): 68.70.+w, 61.43.Hv, 02.70.Rr, 87.15.Nn

I. INTRODUCTION

The simplest and the most intriguing class of stochastic algorithms simulating nonequilibrium Laplacian systems is the diffusion-limited aggregation (DLA) model originally introduced by Witten and Sander [1,2]. Since its introduction in 1981, this model has motivated many investigations devoted to the mathematical description and characterization of growing clusters as well as to numerical simulations of natural processes such as viscous fingering, electrodeposition, dielectric breakdown, dissolution of porous materials, and formation of dendrites and dendrimers [3–10]. However, some details of DLA fundamentals are still far from clear, especially those relevant to asymptotic problems of pattern formation [11–15].

One of the most important DLA puzzles deals with the morphological crossover from ramified to dendritelike clusters as one replaces the original Witten-Sander algorithm by various multiple-hit averaging schemes that are applied to decrease stochastic noise [16–20]. This poses the following major question formulated by Meakin and co-workers [21,22]: can we consider the resulting ''noise-reduced'' shapes to provide statistical properties of the original DLA clusters? Although the multiple-hit averaging schemes are generally accepted and widely used in numerical simulations, their adequacy to the DLA issue needs further theoretical justification. In this connection, particularly obscure is the effect of the cluster anisotropy which systematically appears in on-lattice simulations and then is enhanced considerably as one increases the intensity of averaging [16–27]. Although this anisotropy enhancement, in itself, is not surprising (since it has a rather clear phenomenological explanation [23,24] and can be excluded by a modification of boundary conditions [12]), it adds to the serious reasons to investigate and compare long-range statistics of the original and dendritelike DLA patterns.

In the present work, we try to clarify the formulated problem of noise reduction by analysis of the long-range correlation of the symmetry broken at the microscopic level via the introduction of a chirality to the ordinary Witten-Sander DLA model. Our theory is based on the concept of asymmetric conditions of aggregation—instead of circular growth units, we consider each of them to consist of a chiral (i.e., characterized by the absence of left-right symmetry) combination of microblocks. We demonstrate that both the original and the noise-reducing DLA algorithms are asymptotically achiral, yielding an additional argument that the multiple-hit averaging does not break the original balance between deterministic and stochastic forces governing the long-range statistics of the DLA model. The paper is organized as follows. In Sec. II, we introduce general principles of the microchiral DLA algorithm. Then Secs. III and IV describe extensive Monte Carlo simulations and subsequent chiral analysis of the clusters grown in off- and on-square-lattice conditions, respectively. Finally, Sec. V gives a discussion of the results obtained and formulates the conclusions.

II. GENERAL FORMULATION

Let us assume a DLA process taking place in two-dimensional (2D) open geometry $\mathbf{r}=(x,y)$ with a circular source of walkers outside a cluster placed at the origin (0,0) initially. A walker released from the source obeys simple random wandering until it aggregates onto a position somewhere on the cluster surface. The only difference from the ordinary Witten-Sander DLA model consists in a modification of the neighborhood conditions determining the geometry of aggregation. We consider the walker as a particle whose image in the mirror plane cannot be brought to coincide with itself, i.e., it demonstrates 2D chirality. In this work, we choose one of the simplest chiral shapes, shown in Fig. 1. The structure involves five microblocks combined in chiral $\wr$-like way; each microblock is a circular unit of diameter d.

*Electronic address: bogoyavlenskiy@usa.net

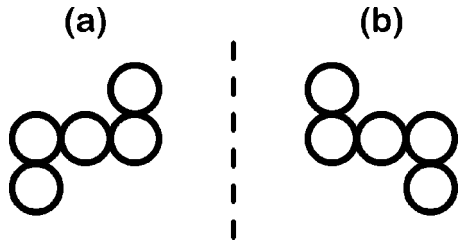

FIG. 1. Chiral walker (a) shown with its image (b) in the mirror plane (dashed line); the structures represent asymmetric junctions of five circular microblocks of diameter d.

In order to investigate and describe chiral properties of DLA clusters on different (micro-, meso-, and macroscopic) length scales, we construct a measure based on the local orientation of walker attachment. For a new walker sticking onto the cluster surface, let $\mathbf{r}'$ and $\mathbf{r}$ be the vectors from the cluster origin to the positions of the attached walker and its ''parent'' in the aggregate (upon which the attachment occurs), respectively; we consider here the position of a particle to be related to its center. Then the vector $\mathbf{r}$ sets the radial direction of the elementary act of aggregation, whereas the parameter $\mathbf{r}_0 \equiv \mathbf{r}' - \mathbf{r}$ determines the local sticking orientation. We define the angle of attachment $\varphi \in [-180°, 180°]$ to be measured counterclockwise from $\mathbf{r}$ to $\mathbf{r}_0$. In description of the particle ensemble forming a DLA cluster, we focus on the probability $P(\varphi, r)$ giving a distribution of the attachment angle φ for the particles located in a neighborhood of the circle of radius $r \equiv |\mathbf{r}|$; the function $P(\varphi, r)$ is considered to satisfy the normalization condition on φ

$$\int_{-180°}^{180°} P(\varphi, r)\, d\varphi = 1 \quad \forall r. \tag{1}$$

The probability distribution $P(\varphi, r)$ defined above provides the following quantitative measure of chirality:

$$\overline{\varphi}(r) \equiv \int_{-180°}^{180°} \varphi P(\varphi, r)\, d\varphi. \tag{2}$$

The function $\overline{\varphi}(r)$ determines the average angle of attachment for the particles located at distance r from the cluster origin. If the distribution $P(\varphi, r)$ demonstrates an asymmetric behavior on angle inversion, i.e., $P(\varphi, r) \neq P(-\varphi, r)$, then the average angle $\overline{\varphi}(r) \neq 0$. This local parameter of chirality $\overline{\varphi}(r)$ can be generalized for the whole DLA cluster, producing the measure usually called the *rotatory power*,

$$\Phi(R) \equiv \frac{D}{R^D} \int_0^R r^{D-1} \overline{\varphi}(r)\, dr, \tag{3}$$

where R is the radius of gyration and D is the fractal dimension of the cluster. The absolute value of the rotatory power $\Phi(R)$ can be used to assess whether one cluster is more or less chiral than another; the sign of $\Phi(R)$ describes the handedness assigned to the aggregate.

In our Monte Carlo simulations, the chiral walkers [Fig. 1(a)] are launched at a random position on a circle of radius $R + 10d$ and are lost if the distance to the cluster origin exceeds the critical value of $2(R + 10d)$. Since the diffusing particles are asymmetric, each walker is characterized, except for the position of its center, by a polar angle α, the orientation parameter relative to the coordinate basis. We consider this orientation angle to be either uniformly distributed in the range $\alpha \in [0°, 360°]$ (for off-lattice simulations) or chosen from the discrete set $\alpha \in \{0°, 90°, 180°, 270°\}$ (for on-square-lattice algorithms) when a walker is released from the source, and then to keep its initial value during the wandering until aggregation occurs. Following this procedure, we investigated the chiral parameters $[P(\varphi, r)$, $\overline{\varphi}(r)$, and $\Phi(R)]$ for DLA clusters of radius up to $10^3 d$ that contain up to 12 000 chiral particles. In order to obtain a sufficiently extensive data set for subsequent statistical analysis, we simulated ensembles of 10^2–10^6 clusters for each particular size studied.

III. OFF-LATTICE DLA

For off-lattice simulations of DLA clusters, we have adapted an efficient hierarchical algorithm designed by Tolman and Meakin [28]. The approach consists in constructing a collection of coarse-grained cluster versions at different length scales. First, the cluster as seen at the coarsest scale is examined and, if a jump to a randomly chosen direction on that scale can be taken by the diffusing walker, the jump is executed. Otherwise, one switches to the next lower scale to get more accurate information about the location of the cluster in the vicinity of the walker. This process of consulting more and more resolved approximations continues until one reaches the lowest scale. At this level, one knows whether the diffusing walker has already contacted the cluster or if it can be moved by a small distance. After a new particle has been added to the DLA cluster, the collection of hierarchical coarse-grained data is updated.

An overall picture for the off-lattice DLA model with chiral particles is summarized by Figs. 2 and 3. In Fig. 2(a), we present the computed dependence of the probability distribution $P(\varphi, r)$ on the angle of attachment $\varphi \in [-180°, 180°]$ for the following three values of the distance from the cluster origin: $r = 5d$, $50d$, and $500d$. The data obtained demonstrate a qualitative resemblance to the results reported for the ordinary DLA model with circular particles [29,30]; the curves are satisfactorily approximated by cosine functions as

$$P(\varphi, r) = \frac{1}{360°} + A(r)\cos(\varphi), \tag{4}$$

where the constant 1/360° ensures the normalization condition [Eq. (1)] and the parameter $A(r)$, being the cosine amplitude, decreases monotonically as the distance r enlarges. This fitting formula mimics the fact that, in the DLA model, the forward sticking of walkers dominates the backward sticking, especially for small cluster size. The deviations from Eq. (4) become remarkable only when the distance from the cluster origin r is comparable with the particle di-

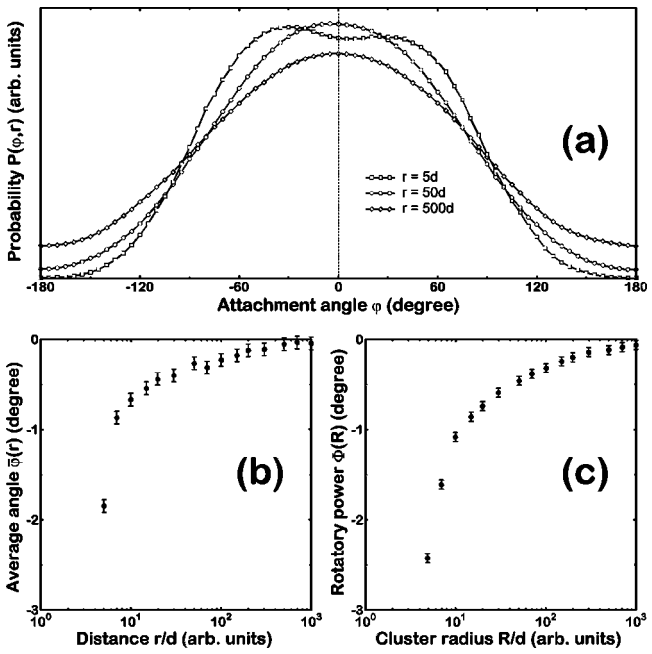

FIG. 2. Statistical analysis of the chiral off-lattice DLA model. (a) Probability distribution $P(\varphi,r)$ vs angle of attachment $\varphi \in [-180°,180°]$ for the following three distances from the cluster origin: $r/d=5$, 50, and 500; each curve is calculated by the averaging of a 10^6-particle ensemble. (b) Average angle of attachment $\overline{\varphi}$ vs distance from the cluster origin $r/d \in [5,1000]$ on a logarithmic scale; statistical errors of data are $\pm 0.07°$. (c) Rotatory power Φ vs cluster radius $R/d \in [5,1000]$ on a logarithmic scale; statistical errors of data are $\pm 0.04°$.

ameter d; a peak of the probability distribution $P(\varphi,r)$ as $\varphi=0°$ observed at $r=500d$ and $50d$ splits into two maxima for the curve $r=5d$.

The parameters of chirality $\overline{\varphi}(r)$ and $\Phi(R)$ calculated from the probability distribution $P(\varphi,r)$ with use of Eqs. (2) and (3) are presented in Figs. 2(b) and 2(c), respectively. The dependence of the average angle $\overline{\varphi}$ on the distance from the cluster origin r shown in Fig. 2(b) originates from a value of several degrees in the clockwise direction as the cluster initiates its growth. The subsequent increase of r results in progressive decrease of the absolute value of $\overline{\varphi}$ to zero; $|\overline{\varphi}(r)|$ becomes comparable with the statistical error $\pm 0.07°$ as the distance r exceeds $500d$. As seen from Fig. 2(c), the dependence of the rotatory power Φ on the cluster radius R obtained from integration of the average angle $\overline{\varphi}(r)$ is similar to the evolution $\overline{\varphi}$ of r [Fig. 2(b)]. The main conclusion we can draw from these two plots is that the functions $\overline{\varphi}(r)$ and $\Phi(R)$ are extrapolated to zero in the limits $r\to\infty$ and $R\to\infty$, respectively, i.e., the off-lattice DLA model with chiral particles is asymptotically achiral. Indeed, an insignificant initial chirality resolved for small clusters $R/d<10^1$ progressively fades as one proceeds to larger scale $R/d>10^2$. This absence of macroscopic chirality is illustrated by Fig. 3 which presents a typical DLA cluster of radius $R=10^3d$. The pattern obtained looks like a regular DLA cluster simulated by the original Witten-Sander off-lattice algorithm [31].

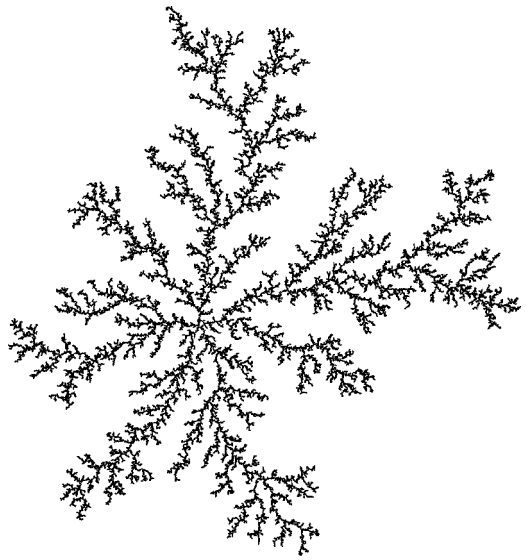

FIG. 3. Typical off-lattice DLA cluster consisting of 12 000 chiral particles; gyration radius $R\approx 10^3d$.

IV. ON-LATTICE DLA

For on-lattice Monte Carlo simulations, we take a square grid of spacing d relevant to the imposed structure of the chiral walker [Fig. 1(a)]. The corresponding transformation of the off-lattice algorithm includes the following simplifications: (i) the wandering of walkers is restricted to the $\langle 10\rangle$, $\langle \overline{1}0\rangle$, $\langle 01\rangle$, and $\langle 0\overline{1}\rangle$ crystallographic directions, i.e., we consider nearest-neighborhood conditions of aggregation; (ii) the angle of particle orientation α is randomly chosen with equal probability from the four values 0°, 90°, 180°, and 270° (the latter two angles, 180° and 270°, are identical with 0° and 90°, respectively, due to the center symmetry of the walkers); (iii) finally, the hierarchical coarse-grained scheme [28] is reduced to the classic Witten-Sander algorithm [1].

A. No noise reduction

The substitution of the on-square lattice conditions for the off-lattice chiral DLA model gives the results summarized by Figs. 4, 5, and 6. In Fig. 4, we present (i) the probability distribution $P(\varphi,r)$ as a function of $\varphi\in[-180°,180°]$ for the same three distances from the cluster origin as in the off-lattice algorithm: $r=5d$, $50d$, and $500d$ [Fig. 4(a)], (ii) the average angle of attachment $\overline{\varphi}(r)$ [Fig. 4(b)], and (iii) the rotatory power $\Phi(R)$ [Fig. 4(c)]. The data obtained show that the introduced microchirality yields only a slight mesochirality for clusters of small size; the rotatory power Φ is characterized by values of $\approx 1°$ in the counterclockwise direction at $R=10d$. This chiral behavior at mesoscale, however, is progressively lost as the radius of gyration R increases further, to the benefit of cluster growth. As a consequence, the on-square lattice DLA model with chiral particles is asymptotically achiral like the off-lattice one. Actually, the typical cluster of radius $R=10^3d$ shown in Fig. 5

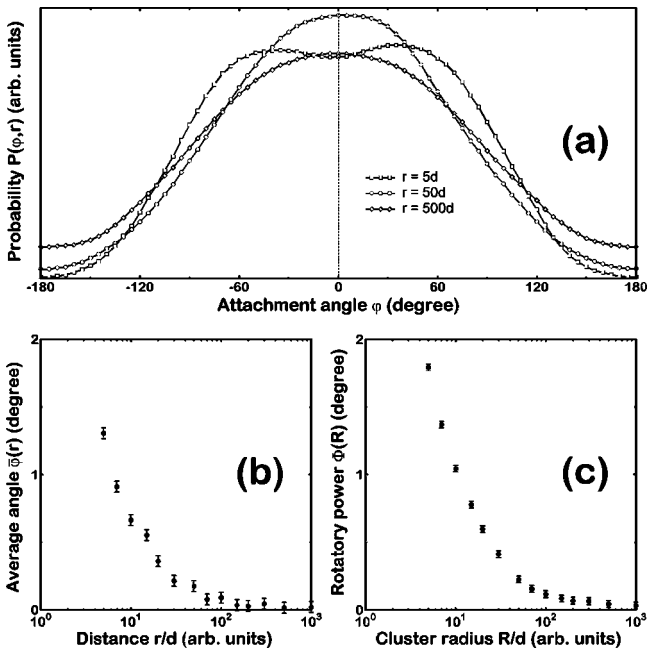

FIG. 4. Statistical analysis of the chiral DLA model on a square lattice (d is the grid spacing) in the case of the original nonaveraging algorithm. (a) Probability distribution $P(\varphi,r)$ vs angle of attachment $\varphi\in[-180°,180°]$ for the following three distances from the cluster origin: $r/d=5$, 50, and 500; each curve is calculated by the averaging of a (4×10^6)-particle ensemble. (b) Average angle of attachment $\bar{\varphi}$ vs distance from cluster origin $r/d\in[5,1000]$ on a logarithmic scale; statistical errors of data are $\pm0.04°$. (c) Rotatory power Φ vs cluster radius $R/d\in[5,1000]$ on a logarithmic scale; statistical errors of data are $\pm0.02°$.

does not illustrate any chiral properties at macroscopic scale, looking similar to the corresponding off-lattice pattern (Fig. 3).

In order to study the spatial distribution of the grown cluster ensemble, we have calculated the mean occupancy

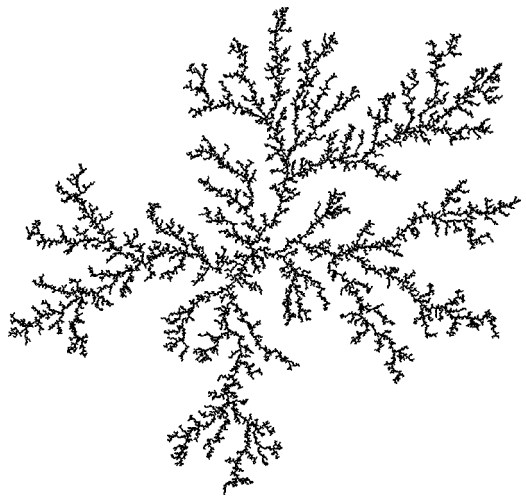

FIG. 5. Typical DLA cluster on square lattice (d is the grid spacing) in case of the original nonaveraging algorithm; the cluster consisting of 12 000 chiral particles is grown up to gyration radius $R\approx10^3d$.

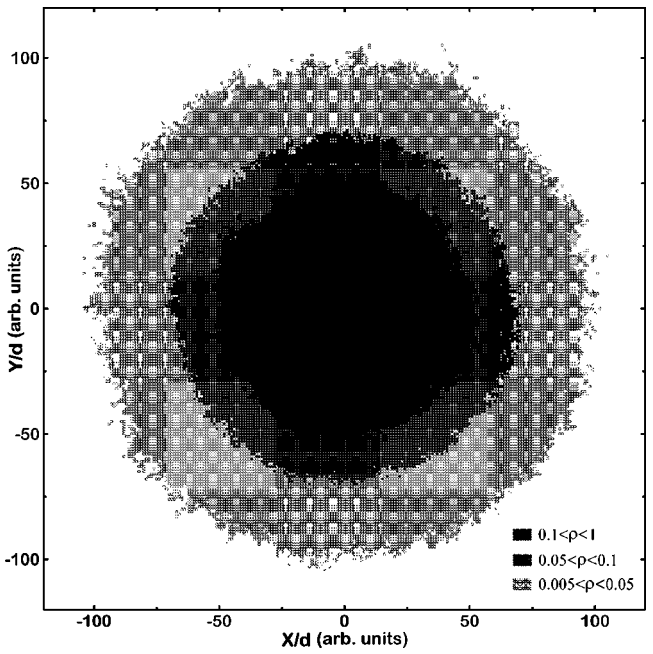

FIG. 6. Field-plot representation of the mean cluster occupancy $\rho(x,y)$ for the chiral DLA model on a square lattice (d is the grid spacing) in the case of the original nonaveraging algorithm. These data are computed from ensemble averaging over 2500 clusters of radius $R\approx10^2d$ consisting of 400 chiral particles; the fields are $0.005\leqslant\rho<0.05$, $0.05\leqslant\rho<0.1$, and $0.1\leqslant\rho<1$ from the outer to the inner.

function $\rho(x,y)$ presented in Fig. 6. The obtained contour plots of $\rho(x,y)$ are close to concentric circles, thus additionally demonstrating the achiral and isotropic properties of the chiral on-lattice DLA algorithm.

B. Noise reduction

The effect of ''noise reduction'' is achieved when one applies multiple-hit averaging to the DLA model. The generalization is based on the original DLA algorithm [1] in which a walker wanders on the lattice until it sticks onto a position at the cluster surface, but instead of immediate aggregation of that walker to the cluster, one adds unity to a counter of the walker site corresponding to the surface position; when the counter exceeds a predetermined value $N_C\geqslant2$, the walker site is considered to be occupied. There are the two following variations of the averaging procedure: (i) the multiple-hit scheme with erasing, in which the counters on all other sites are dropped to zero as a new particle is added to the cluster, and (ii) the multiple-hit scheme without erasing, also called the Tang algorithm [32], in which the counters accumulate the number of walker visits during the whole aggregation process.

1. Multiple hits with erasing

For this noise-reducing modification of the DLA model, we investigated two- and four-hit averaging schemes, i.e., with $N_C=2$ and $N_C=4$, respectively; the results obtained are summarized by Figs. 7 and 8. In Fig. 7, we illustrate evolution of the probability distribution $P(\varphi,r)$ [Figs. 7(a)

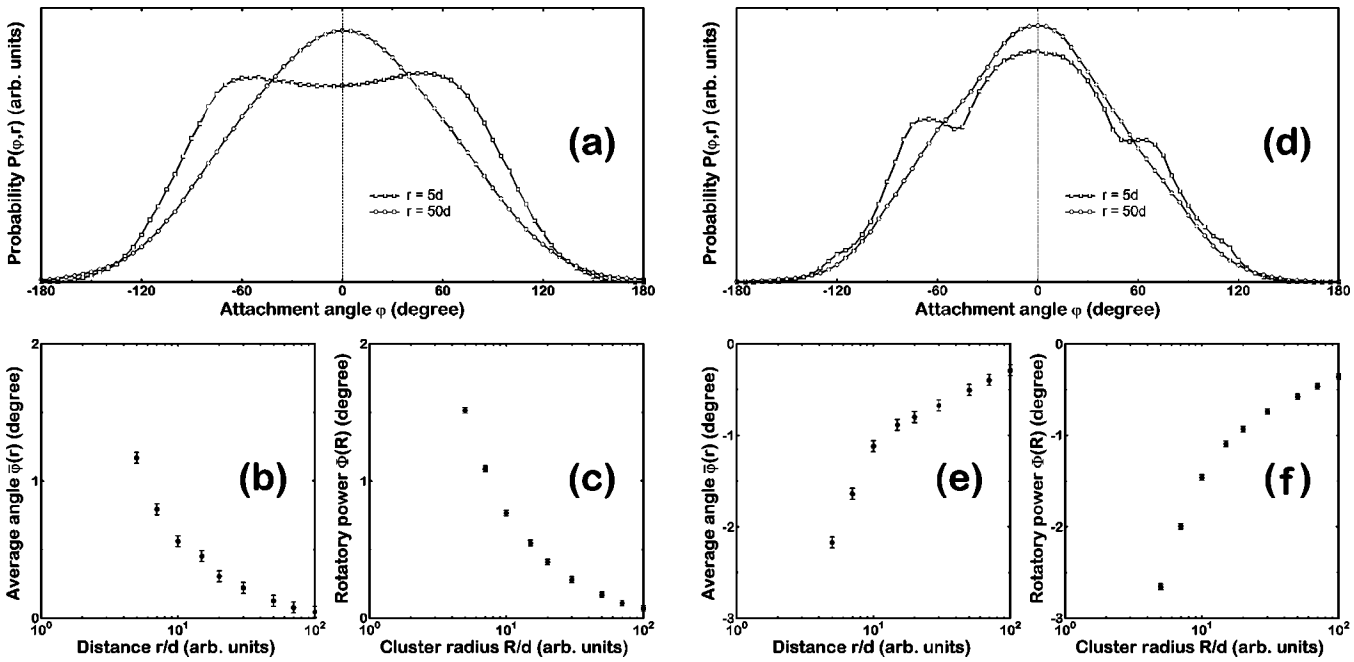

FIG. 7. Statistical analysis of the chiral DLA model on a square lattice (d is the grid spacing) in case of the multiple-hit algorithm with erasing; parameter of averaging $N_C=2$ [plots (a), (b), and (c)] or $N_C=4$ [plots (d), (e), and (f)]. (a) and (d) Probability distribution $P(\varphi,r)$ vs angle of attachment $\varphi\in[-180°,180°]$ for the following two distances from the cluster origin: $r/d=5$ and 50; each curve is calculated by the averaging of a (4×10^5)-particle ensemble. (b) and (e) Average angle of attachment $\overline{\varphi}$ vs distance from the cluster origin $r/d\in[5,100]$ on a logarithmic scale; statistical errors of data are $\pm0.06°$. (c) and (f) Rotatory power Φ vs cluster radius $R/d\in[5,100]$ on a logarithmic scale; statistical errors of data are $\pm0.03°$.

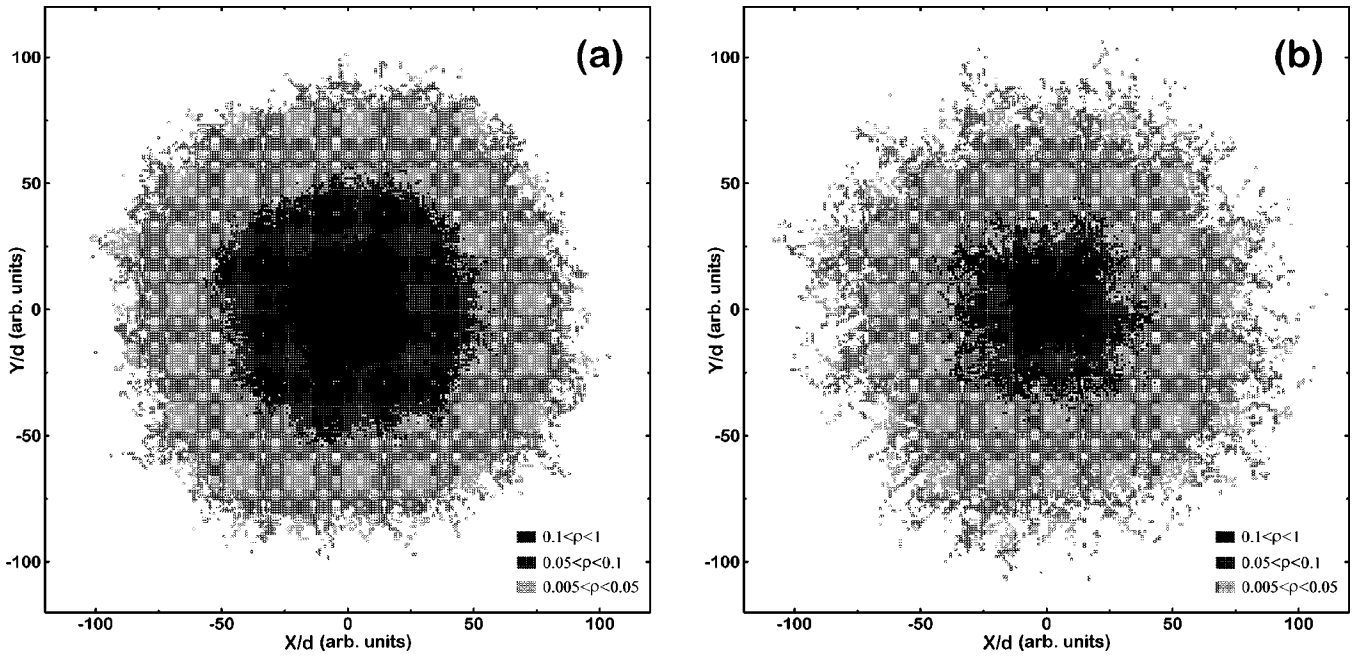

FIG. 8. Field-plot representation of the mean cluster occupancy $\rho(x,y)$ for the chiral DLA model on a square lattice (d is the grid spacing) in case of the multiple-hit algorithm with erasing; parameter of averaging $N_C=2$ (a) or $N_C=4$ (b). These data are computed from ensemble averaging over 1000 clusters of radius $R\approx10^2d$ consisting of 200 (a) or 100 (b) chiral particles; the fields are $0.005\leqslant\rho<0.05$, $0.05\leqslant\rho<0.1$, and $0.1\leqslant\rho<1$ from the outer to the inner.

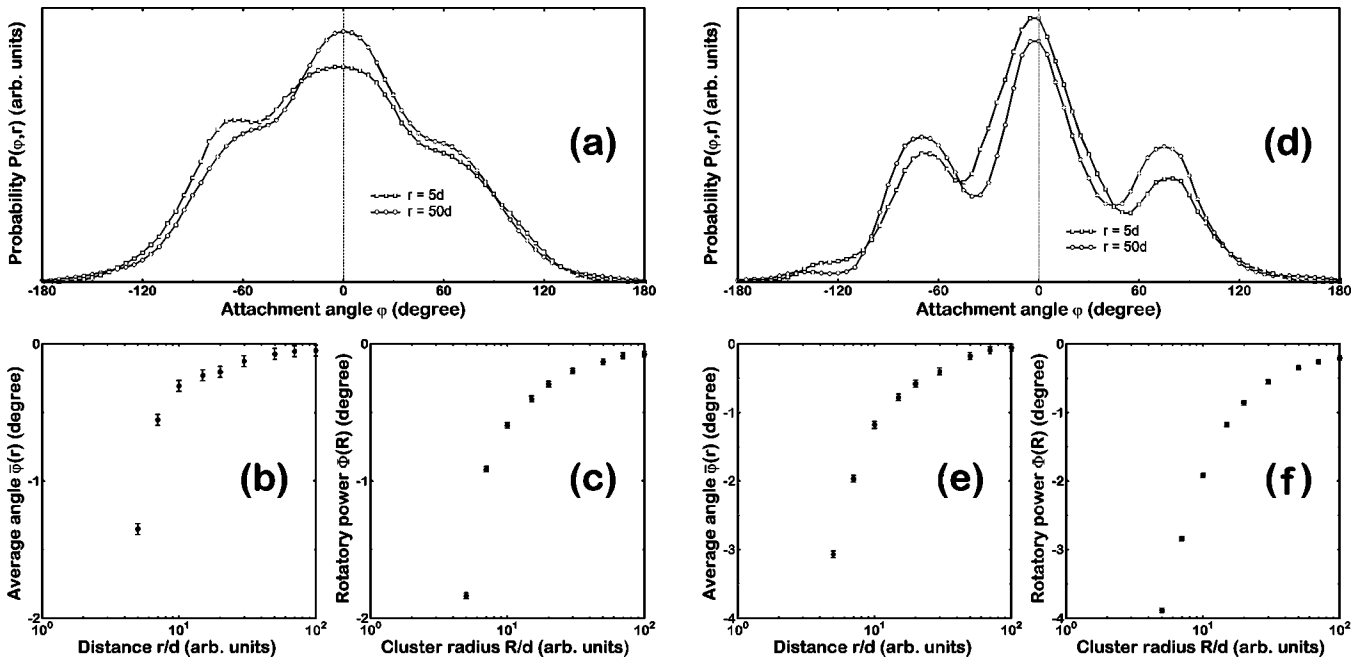

FIG. 9. Statistical analysis of the chiral DLA model on a square lattice (d is the grid spacing) in the case of the multiple-hit algorithm without erasing (the Tang scheme); parameter of averaging $N_C=4$ [plots (a), (b), and (c)] or $N_C=16$ [plots (d), (e), and (f)]. (a) and (d) Probability distribution $P(\varphi,r)$ vs angle of attachment $\varphi\in[-180°,180°]$ for the following two distances from the cluster origin: $r/d=5$ and 50; each curve is calculated by the averaging of a 10^6-particle ensemble. (b) and (e) Average angle of attachment $\overline{\varphi}$ vs distance from the cluster origin $r/d\in[5,100]$ on a logarithmic scale; statistical errors of data are $\pm 0.04°$. (c) and (f) Rotatory power Φ vs cluster radius $R/d\in[5,100]$ on a logarithmic scale; statistical errors of data are $\pm 0.02°$.

and 7(d)], of the average angle of attachment $\overline{\varphi}(r)$ [Figs. 7(b) and 7(e)], and of the rotatory power $\Phi(R)$ [Figs. 7(c) and 7(f)] caused by the variation of parameter N_C. One can resolve the following changes as the averaging intensity increases: (i) the forward-aggregating direction, $\varphi=0°$, becomes preferable, so angle dispersion of the probability distribution $P(\varphi,r)$ slightly decreases; (ii) some peculiarities at $\varphi\approx\pm 70°$ are revealed in the curves $P(\varphi,r)$, corresponding to the secondmost preferable aggregation, with respect to the main forward orientation; (iii) as a rather surprising result, the chiral parameters $\overline{\varphi}(r)$ and $\Phi(R)$ demonstrate sign inversion from the counterclockwise direction (relevant to the on-lattice algorithm without noise reduction) to the clockwise one as N_C increases from 2 to 4. An insignificant chirality observed for small clusters $R<10d$ then successfully fades at the macroscopic scale. Thus, the results of the multiple-hit scheme with erasing qualitatively resemble the results for the nonaveraging algorithm (Fig. 4).

Additional information characterizing the crossover from the original DLA to this noise-reducing scheme is shown in Fig. 8, which presents the mean cluster occupancy distributions $\rho(x,y)$ for $N_C=2$ [Fig. 8(a)] and $N_C=4$ [Fig. 8(b)]. The imposed averaging results in the appearance of a radial anisotropy of $\rho(x,y)$: the isotropic (or quasi-isotropic) distribution of the mean occupancy corresponding to the nonaveraging algorithm (Fig. 6) transforms here to an anisotropic pattern with fourfold symmetry rotated by the angle $\beta\approx 37°$ in the clockwise direction, relative to the coordinate basis [33]. This appearance of growth axes is not, however, accompanied by a development of chirality at the macroscale, which is actually absent, as also follows from Fig. 8.

2. Multiple hits without erasing

The application of the other modification of the multiple-hit averaging (the Tang procedure) to the chiral DLA model is summarized by Figs. 9 and 10; here we give the results for $N_C=4$ and $N_C=16$. In Fig. 9, the probability distribution $P(\varphi,r)$ [Figs. 9(a) and 9(d)], the average angle of attachment $\overline{\varphi}(r)$ [Figs. 9(b) and 9(e)], and the rotatory power $\Phi(R)$ [Figs. 9(c) and 9(f)] are presented. The figure shows that the Tang scheme, as well as the multiple hits with erasing (Fig. 7), causes decrease of the angle dispersion of the probability $P(\varphi,r)$; this leads to the same peculiarities in the curves $P(\varphi,r)$ at $\varphi\approx\pm 70°$ clearly resolved as secondary peaks. As in all the algorithms studied before (Figs. 2, 4, and 7), a slight chirality (in the clockwise direction) is reported for clusters of mesoradius and then disappears as one proceeds to macroscopic scale.

The analysis of the mean cluster occupancy $\rho(x,y)$ presented in Fig. 10 for $N_C=4$ [Fig. 10(a)] and $N_C=16$ [Fig. 10(b)] reveals the achiral and anisotropic properties of the produced patterns that qualitatively repeat the results of the multiple-hit averaging with erasing (Fig. 8). As the main difference from Fig. 8, Tang's averaging leads to DLA clusters that are more anisotropic along the preferential growth directions determined as $\pi n/2-\beta$, $n=\{0,1,2,3\}$ [33].

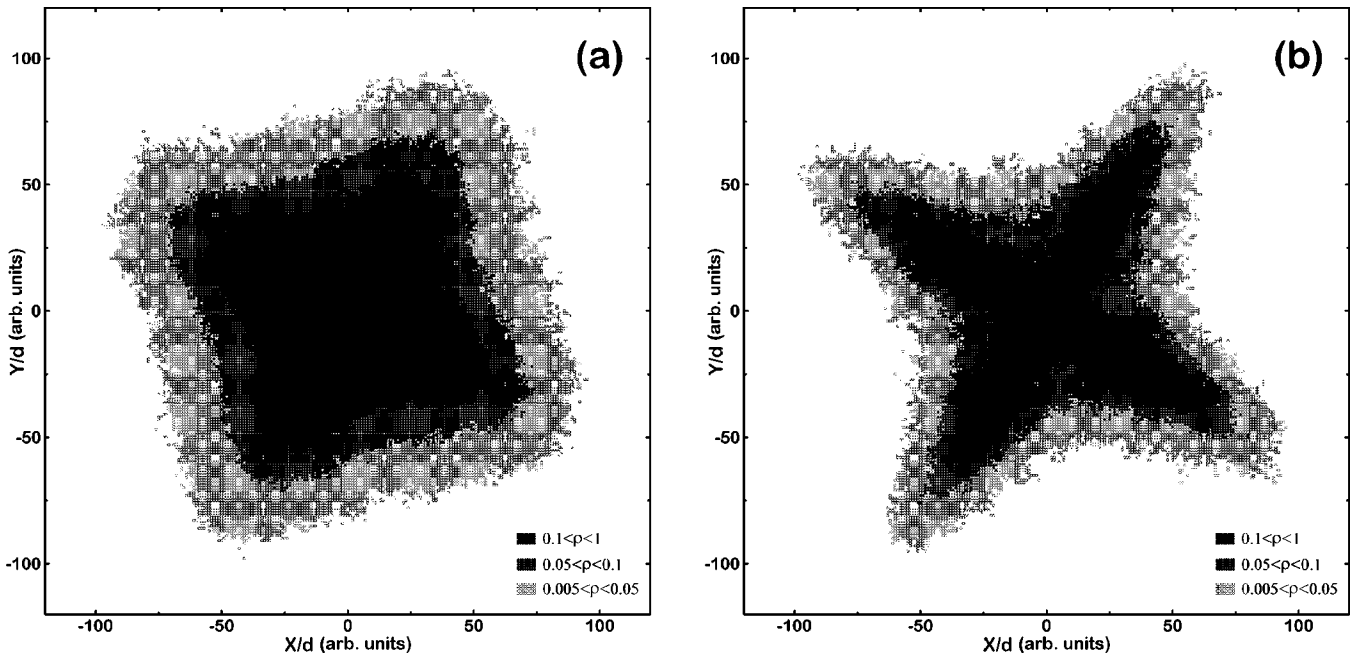

FIG. 10. Field-plot representation of the mean cluster occupancy $\rho(x,y)$ for the chiral DLA model on a square lattice (d is the grid spacing) in case of the multiple-hit algorithm without erasing (the Tang scheme); parameter of averaging $N_C=4$ (a) or 16 (b). These data are computed from ensemble averaging over 1000 clusters of radius $R\approx 10^2 d$ consisting of 350 (a) or 300 (b) chiral particles; the fields are $0.005\leqslant\rho<0.05$, $0.05\leqslant\rho<0.1$, and $0.1\leqslant\rho<1$ from the outer to the inner.

V. DISCUSSION AND CONCLUSIONS

Let us summarize the statistical investigations of the DLA model performed and described in the previous two sections. The most important result we obtained is that the introduction of microchirality into the ordinary Witten-Sander formulation does not, remarkably, yield a chiral behavior of growing clusters at the macroscopic length scale for either the original DLA algorithm or various multiple-hit averaging schemes. What does this mean, how can we explain it, and what can we conclude? These are the topics of this section.

Before we start to discuss the questions posed above, let us review a general natural picture. In spite of the variety of growth structures observed in non-equilibrium Laplacian-type systems [3–10], the formation of chiral patterns is reported only for a small number of objects such as liquid crystals [34,35], bacterial colonies [36–39], and fullerene-based films [40,41]. However, the vast majority of growth units demonstrate a significant asymmetry at the microscopic level consistent with geometric or kinetic factors—typical examples vary from chiral carbon chains in organic molecules [42] to the complex collective behavior of bacteria [43].

This natural disparity between micro- and macroasymmetry (or symmetry) is closely associated with the theoretical problem of the balance between deterministic and stochastic forces in growth processes that are far from equilibrium. Indeed, the chirality here plays the role of an order/disorder parameter, the scale evolution of which can be quantitatively studied, e.g., by rotatory power measurements. Thus the DLA model, the principal representation of nonequilibrium, diffusive, and fractal growth, is of fundamental importance.

In order to analyze the DLA mechanism in detail, one needs to cut the Gordian knot of deterministic and stochastic contributions, which both affect the process. The DLA deterministic part can be described separately from the stochastic part—it is the quasi-steady-state approximation of the full diffusion problem [12]:

$$\nabla^2 F(\mathbf{r})=0, \tag{5}$$

$$F(\mathbf{r})\big|_{\mathbf{r}\in\overline{\mathbf{r}}}=F_0(\mathbf{r}), \tag{6}$$

$$V_n\big|_{\mathbf{r}\in\overline{\mathbf{r}}_c}=\Gamma(\nabla F\cdot\mathbf{n}\big|_{\mathbf{r}\in\overline{\mathbf{r}}_c}). \tag{7}$$

Here $F(\mathbf{r})$ is the growth potential (e.g., energy density, concentration, etc.) satisfying the Laplace equation (5); $F_0(\mathbf{r})$ is a given function that implies the Dirichlet condition (6) on the boundary $\mathbf{r}\in\overline{\mathbf{r}}$; the symbol $\overline{\mathbf{r}}_c$ denotes the interface part of the whole boundary, on which the conservation law (7) is imposed; $\mathbf{n}$ is the unit normal, V_n is the normal growth speed, and Γ is a constant determined by diffusivity and other physical parameters.

As follows from this general formulation [Eqs. (5)–(7)], the deterministic contribution of DLA is strongly influenced by asymmetry in aggregation conditions on the interface. The imposed geometrical chirality of the walkers definitely implies chiral properties of Eq. (7) arising from asymmetric behavior of the normal vector $\mathbf{n}$. In other words, if the DLA model was a fully deterministic process, our introduction of microchirality would result in chiral patterns at macroscopic length scale as well as at mesoscale. The absence of clearly resolved macrochirality allows us to draw the conclusion that, in the superposition of deterministic and stochastic DLA forces, the random contribution is dominating. The

domination here is considered as a short-range loss of memory about local growth conditions.

The weak long-range correlation of symmetry revealed in the DLA-produced clusters is not, in principle, a self-evident property caused by the fractal scaling. For the simplest counterexample, we can discuss the other class of stochastic growth algorithms based on the Eden model [44]. In this process, a fractal cluster is formed by the appearance of new branches originating from any of the particles of that cluster with a given probability (the variable parameter). As pointed out by Ben-Jacob and co-workers [36,37], the introduction of chirality into the mechanism of an Eden-type sidebranching combined with artificial nutrient laws results in a numerical scheme that satisfactorily simulates the behavior of the bacterium *Bacillus subtilis*, known to form chiral colonies. The self-similar patterns produced maintain the initial microchirality independently of length scale, demonstrating the domination of local growth rules over statistical randomness, in contrast with the DLA model.

There exists a point of view that multiple-hit averaging applied to the Witten-Sander DLA algorithm should lead to noise reduction, i.e., the original stochastic nature of DLA is reduced and the randomness of growing clusters is decreased. A reasonable justification focuses on the lattice anisotropy being considered as a parameter of order; then the known enhancement of the anisotropy, a result of the multiple-hit schemes, is generally explained as a more deterministic behavior of the model. This theory seems nevertheless to have the following serious gap—the appearance of anisotropy has, as for its background, the very lattice effect caused by various growth paths of walkers aggregating at different crystallographic directions [23,24]. As shown by Johnson and Sekerka [12], this growth anisotropy can be successfully excluded by the introduction of an attachment probability depending on crystallographic orientation and averaging intensity, so the problem raised still remains unclear.

Based on the possible connection of multiple-hit averaging and DLA determinism, one may expect a substantial increase of the deterministic contribution and, therefore, a crossover from achiral (weak long-range correlation) to chiral (stable long-range correlation) shapes when we proceed to the noise-reducing schemes. However, neither the achiral/chiral crossover nor even a significant rise of chirality at mesoscale is experimentally observed; the only difference from the Witten-Sander clusters is that the multiple-hit patterns are more anisotropic and spatially rarefied. Thus we conclude that neither of the averaging algorithms studied (multiple hits with and without erasing) breaks the original balance existing between the deterministic and stochastic forces in the DLA model. We believe this result to be fundamental for all DLA-type statistics.

ACKNOWLEDGMENT

I would like to thank Dr. Natasha Chernova for stimulating discussions and helpful comments.

[1] T.A. Witten and L.M. Sander, Phys. Rev. Lett. **47**, 1400 (1981); Phys. Rev. B **27**, 5686 (1983).
[2] For a review of DLA algorithms, see P. Meakin, in *Phase Transitions and Critical Phenomena*, edited by C. Domb and J.L. Lebowitz (Academic Press, New York, 1988), Vol. 12, pp. 335–489, and references therein.
[3] D. Bensimon, L.P. Kadanoff, S. Liang, B.I. Shraiman, and C. Tang, Rev. Mod. Phys. **58**, 977 (1986).
[4] D.A. Kessler, J. Koplik, and H. Levine, Adv. Phys. **37**, 255 (1988).
[5] J.S. Langer, Science **243**, 1150 (1989).
[6] E. Ben-Jacob and P. Garik, Nature (London) **343**, 523 (1990).
[7] A. Erzan, L. Pietronero, and A. Vespignani, Rev. Mod. Phys. **67**, 545 (1995).
[8] T. Vicsek, *Fractal Growth Phenomena*, 2nd ed. (World Scientific, Singapore, 1992).
[9] P. Meakin, *Fractals, Scaling and Growth Far From Equilibrium* (Cambridge University Press, Cambridge, England, 1997).
[10] *Dendrimers*, edited by F. Vögtle (Springer-Verlag, Berlin, 1998).
[11] I. Yekutieli, B.B. Mandelbrot, and H. Kaufman, J. Phys. A **27**, 275 (1994); B.B. Mandelbrot, H. Kaufman, A. Vespignani, I. Yekutieli, and C.-H. Lam, Europhys. Lett. **29**, 599 (1995); B.B. Mandelbrot, A. Vespignani, and H. Kaufman, *ibid.* **32**, 199 (1995); C.-H. Lam, Phys. Rev. E **52**, 2841 (1995).
[12] B.K. Johnson and R.F. Sekerka, Phys. Rev. E **52**, 6404 (1995).
[13] T.C. Halsey, Phys. Rev. Lett. **72**, 1228 (1994); Europhys. Lett. **39**, 43 (1997); T.C. Halsey, B. Duplantier, and K. Honda, Phys. Rev. Lett. **78**, 1719 (1997).
[14] B. Davidovitch, H.G.E. Hentschel, Z. Olami, I. Procaccia, L.M. Sander, and E. Somfai, Phys. Rev. E **59**, 1368 (1999); B. Davidovich and I. Procaccia, Europhys. Lett. **48**, 547 (1999); E. Somfai, L.M. Sander, and R.C. Ball, Phys. Rev. Lett. **83**, 5523 (1999).
[15] V.A. Bogoyavlenskiy and N.A. Chernova, Phys. Rev. E **61**, 5422 (2000); V.A. Bogoyavlenskiy (unpublished).
[16] J. Nittmann and H.E. Stanley, Nature (London) **321**, 663 (1986).
[17] R.C. Ball, Physica A **140**, 62 (1986).
[18] J. Kertész and T. Vicsek, J. Phys. A **19**, L257 (1986).
[19] P. Meakin, Phys. Rev. A **36**, 332 (1987).
[20] J.-P. Eckmann, P. Meakin, I. Procaccia, and R. Zeitak, Phys. Rev. A **39**, 3185 (1989); Phys. Rev. Lett. **65**, 52 (1990).
[21] P. Meakin, Phys. Rev. A **33**, 3371 (1986).
[22] P. Meakin, R.C. Ball, P. Ramanlal, and L.M. Sander, Phys. Rev. A **35**, 5233 (1987).
[23] R.C. Ball and R.M. Brady, J. Phys. A **18**, L809 (1985).
[24] R.C. Ball, R.M. Brady, G. Rossi, and B.R. Thompson, Phys. Rev. Lett. **55**, 1406 (1985).
[25] F. Family, T. Vicsek, and B. Taggett, J. Phys. A **19**, L727 (1986).
[26] T. Aukrust, M.A. Novotny, D.A. Browne, and K. Kaski, Phys. Rev. A **39**, 2587 (1989).
[27] Y. Couder, F. Argoul, A. Arneodo, J. Maurer, and M. Rabaud,

Phys. Rev. A **42**, 3499 (1990); A. Arneodo, F. Argoul, Y. Couder, and M. Rabaud, Phys. Rev. Lett. **66**, 2332 (1991).
[28] S. Tolman and P. Meakin, Phys. Rev. A **40**, 428 (1989).
[29] R. Hegger and P. Grassberger, Phys. Rev. Lett. **73**, 1672 (1994).
[30] C.-H. Lam, H. Kaufman, and B.B. Mandelbrot, J. Phys. A **28**, L213 (1995).
[31] P. Meakin, Phys. Rev. A **27**, 604 (1983); **27**, 1495 (1983); J. Phys. A **18**, L661 (1985).
[32] C. Tang, Phys. Rev. A **31**, 1977 (1985).
[33] This value of the angle $\beta \approx 37°$ is explained as follows. On the square lattice, the most statistically probable junction of the two chiral particles [Fig. 1(a)] corresponds to the head-to-tail configuration, so the vertical cluster axis (going through the first and third quadrants of the coordinate basis) is formed by a stairlike sequence of microblocks where the width and the height of each ''stair'' is $3d$ and $4d$, respectively. As a result, one obtains $\tan\beta = 3d/4d$, yielding $\beta = \arctan(3/4) \approx 37°$.
[34] P.-G. de Gennes and J. Prost, *The Physics of Liquid Crystals*, 2nd ed. (Oxford University Press, New York, 1993).
[35] A.B. Harris, R.D. Kamien, and T.C. Lubensky, Rev. Mod. Phys. **71**, 1745 (1999).
[36] E. Ben-Jacob, O. Shochet, A. Tenenbaum, I. Cohen, A. Czirók, and T. Vicsek, Nature (London) **368**, 46 (1994); E. Ben-Jacob, I. Cohen, O. Shochet, I. Aranson, H. Levine, and L. Tsimering, *ibid.* **373**, 566 (1995); E. Ben-Jacob, I. Cohen, O. Shochet, A. Tenenbaum, A. Czirók, and T. Vicsek, Phys. Rev. Lett. **75**, 2899 (1995).
[37] E. Ben-Jacob, I. Cohen, and D.L. Gutnick, Annu. Rev. Microbiol. **52**, 779 (1998); E. Ben-Jacob and H. Levine, Sci. Am. **279**, 82 (1998).
[38] I. Golding, Y. Kozlovsky, I. Cohen, and E. Ben-Jacob, Physica A **260**, 510 (1998); I. Cohen, I. Golding, Y. Kozlovsky, and E. Ben-Jacob, Fractals **7**, 235 (1999); Y. Kozlovsky, I. Cohen, I. Golding, and E. Ben-Jacob, Phys. Rev. E **59**, 7025 (1999).
[39] M. Matsushita, J. Wakita, H. Itoh, I. Ràfols, T. Matsuyama, H. Sakaguchi, and M. Mimura, Physica A **249**, 517 (1998); M. Matsushita, J. Wakita, H. Itoh, K. Watanabe, T. Arai, T. Matsuyama, H. Sakaguchi, and M. Mimura, *ibid.* **274**, 190 (1999); M. Mimura, H. Sakaguchi, and M. Matsushita, *ibid.* **282**, 283 (2000).
[40] H.J. Gao, Z.Q. Xue, Q.D. Wu, and S. Pang, J. Mater. Res. **9**, 2216 (1994); Solid State Commun. **97**, 579 (1996).
[41] I.M. Sandler, G.S. Canright, Z. Zhang, H. Gao, Z. Xue, and S. Pang, Phys. Lett. A **245**, 233 (1998); I.M. Sandler, G.S. Canright, H. Gao, S. Pang, Z. Xue, and Z. Zhang, Phys. Rev. E **58**, 6015 (1998).
[42] M. Robinson, *Organic Stereochemistry* (Oxford University Press, Oxford, 2000).
[43] *Bacteria as Multicellular Organisms*, edited by J.A. Shapiro and M. Dworkin (Oxford University Press, New York, 1997).
[44] M. Eden, in *Proceedings of the Fourth Berkeley Symposium on Mathematical Statistics and Probability*, edited by J. Neyman (University of California Press, Berkeley, 1961), Vol. 4, p. 223.